

# Diffraction studies at LHeC and FCC-eh

Anna Staśto



Studies done by **Wojciech Słomiński**, Jagiellonian University, Kraków

# Outline

---

- Introduction: diffraction at HERA
- Phase space for inclusive diffraction at LHeC and FCC-eh
- Reduced cross section - pseudodata simulation
- Simulation of diffractive parton distribution functions
- Diffraction on nuclei

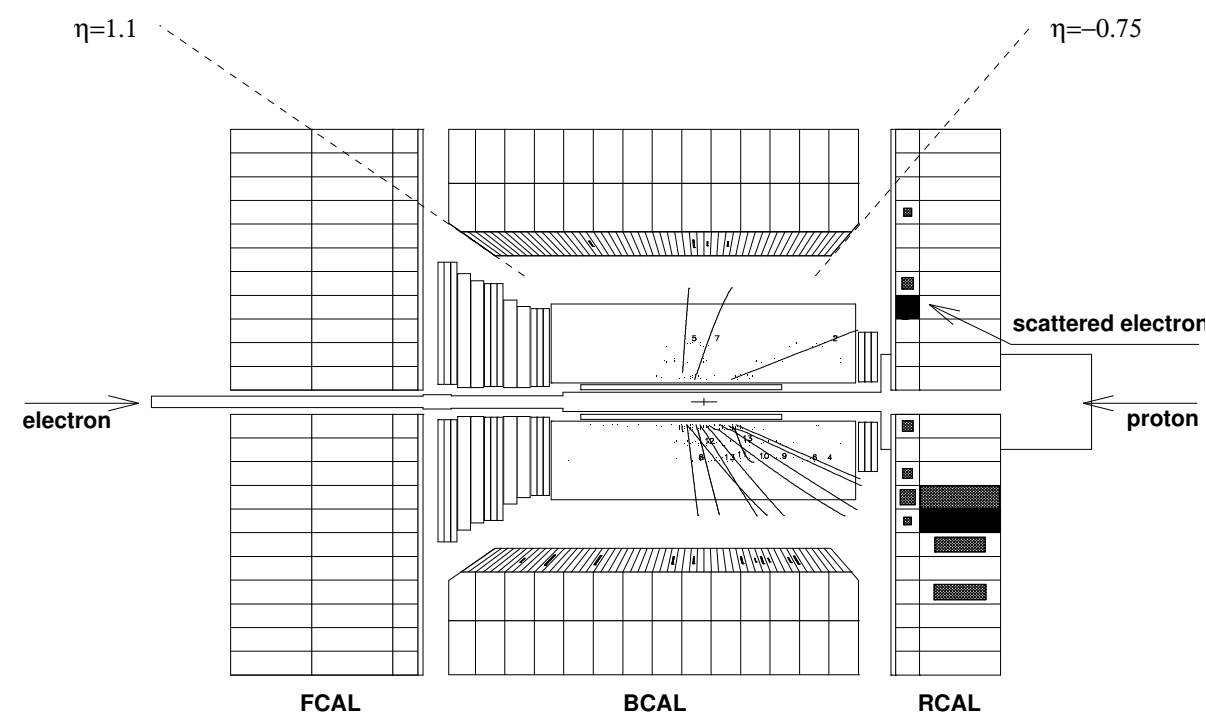
# Introduction

---

## What is diffraction ?

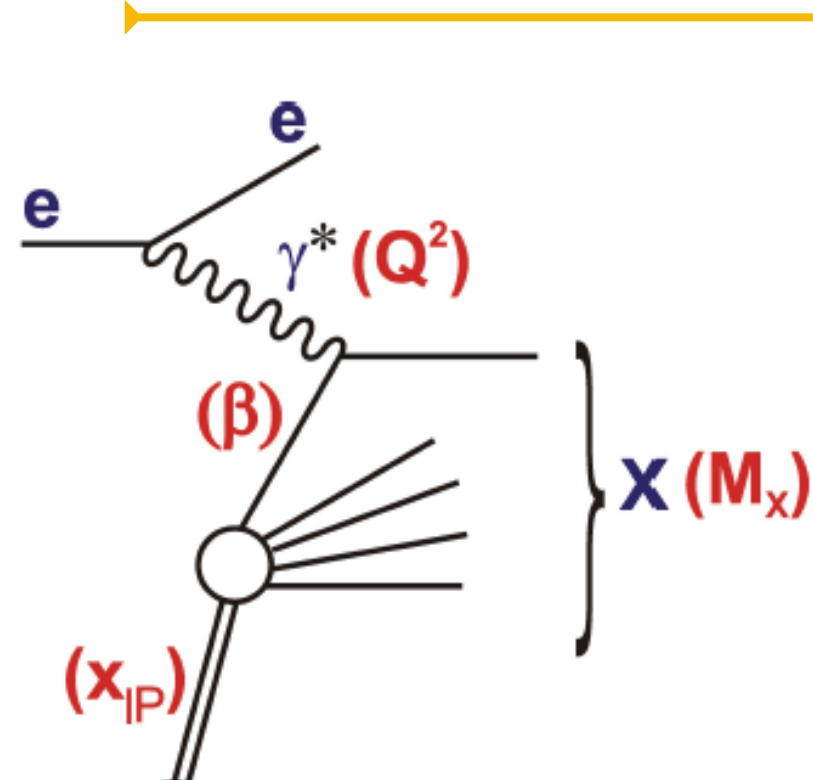
- Diffractive processes are characterized by the rapidity gap: absence of any activity in part of the detector.
- Diffraction is interpreted as to be mediated by the exchange of an ‘object’ with vacuum quantum numbers - usually referred to as the *Pomeron*.

At HERA in electron-proton collisions:  
about 10% events diffractive



Diffractive event in ZEUS at HERA

# Diffractive kinematics in DIS



$$x_{Bj} = x_{IP}\beta$$

## Standard DIS variables:

electron-proton  
cms energy squared:

$$s = (k + p)^2$$

photon-proton  
cms energy squared:

$$W^2 = (q + p)^2$$

inelasticity

$$y = \frac{p \cdot q}{p \cdot k}$$

Bjorken  $x$

$$x = \frac{-q^2}{2p \cdot q}$$

(minus) photon virtuality

$$Q^2 = -q^2$$

## Diffractive DIS variables:

$$\xi \equiv x_{IP} = \frac{Q^2 + M_X^2 - t}{Q^2 + W^2}$$

$$\beta = \frac{Q^2}{Q^2 + M_X^2 - t}$$

$$t = (p - p')^2$$

momentum fraction of  
the Pomeron w.r.t hadron

momentum fraction of  
parton w.r.t Pomeron

4-momentum transfer squared

Two classes of diffractive events in DIS:

$Q^2 \sim 0$  photoproduction

$Q^2 \gg 0$  deep inelastic scattering

# Diffractive structure functions

$$\frac{d^3\sigma^D}{dx_{IP} dx dQ^2} = \frac{2\pi\alpha_{\text{em}}^2}{xQ^4} Y_+ \sigma_r^{D(3)}(x_{IP}, x, Q^2)$$

$$Y_+ = 1 + (1 - y)^2$$

Reduced diffractive cross section depends on two structure functions

$$\sigma_r^{D(3)} = F_2^{D(3)} - \frac{y^2}{Y_+} F_L^{D(3)}$$

For  $y$  not too close to unity we have:

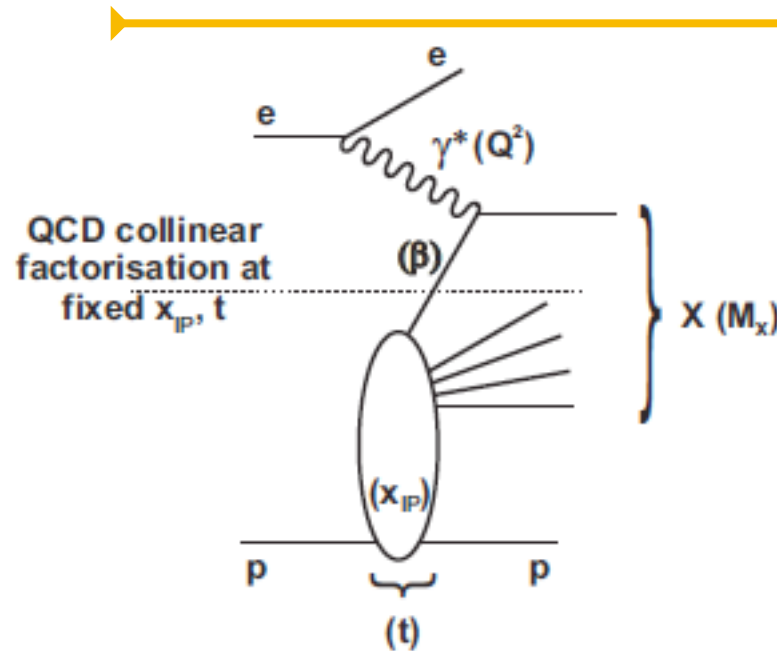
$$\sigma_r^{D(3)} \simeq F_2^{D(3)}$$

Integrated vs unintegrated structure functions over  $t$ :

$$F_{T,L}^{D(3)}(x, Q^2, x_{IP}) = \int_{-\infty}^0 dt F_{T,L}^{D(4)}(x, Q^2, x_{IP}, t)$$

$$F_2^{D(4)} = F_T^{D(4)} + F_L^{D(4)}$$

# Collinear factorization in diffraction



*Collins*  
Collinear factorization in diffractive DIS

$$d\sigma^{ep \rightarrow eXY}(x, Q^2, x_{IP}, t) = \sum_i f_i^D \otimes d\hat{\sigma}^{ei} + \mathcal{O}(\Lambda^2/Q^2)$$

- Diffractive cross section can be factorized into the convolution of the perturbatively calculable partonic cross sections and diffractive parton distributions (DPDFs).
- Partonic cross sections are the same as for the inclusive DIS.
- The DPDFs represent the probability distributions for partons  $i$  in the proton under the constraint that the proton is scattered into the system  $Y$  with a specified 4-momentum.
- Factorization should be valid for sufficiently(?) large  $Q^2$  (and fixed  $t$  and  $x_{IP}$ ).

# DPDF parametrization

Regge factorization (additional assumption)

$$f_i^D(x, Q^2, x_{IP}, t) = f_{IP/p}(x_{IP}, t) f_i(\beta = x/x_{IP}, Q^2)$$

Pomeron flux is parametrized as

$$f_{IP/p}(x_{IP}, t) = A_{IP} \frac{e^{B_{IP}t}}{x^{2\alpha_{IP}(t)-1}}$$

$$\alpha_{IP}(t) = \alpha_{IP}(0) + \alpha'_{IP}t$$

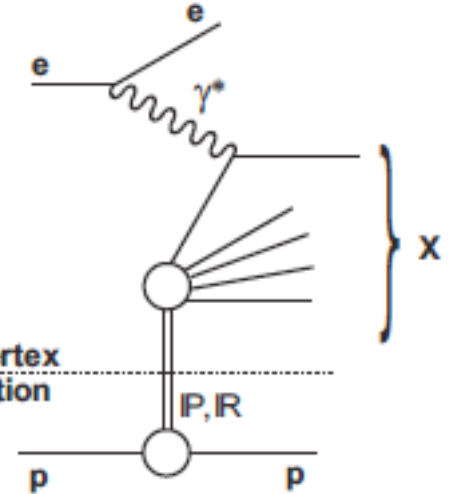
parton distributions in the Pomeron

$$f_k(z) = A_k z^{B_k} (1 - z)^{C_k}$$

where k=g,d. Light quarks equal u=d=s.

For good description of the data usually subleading Reggeons are included

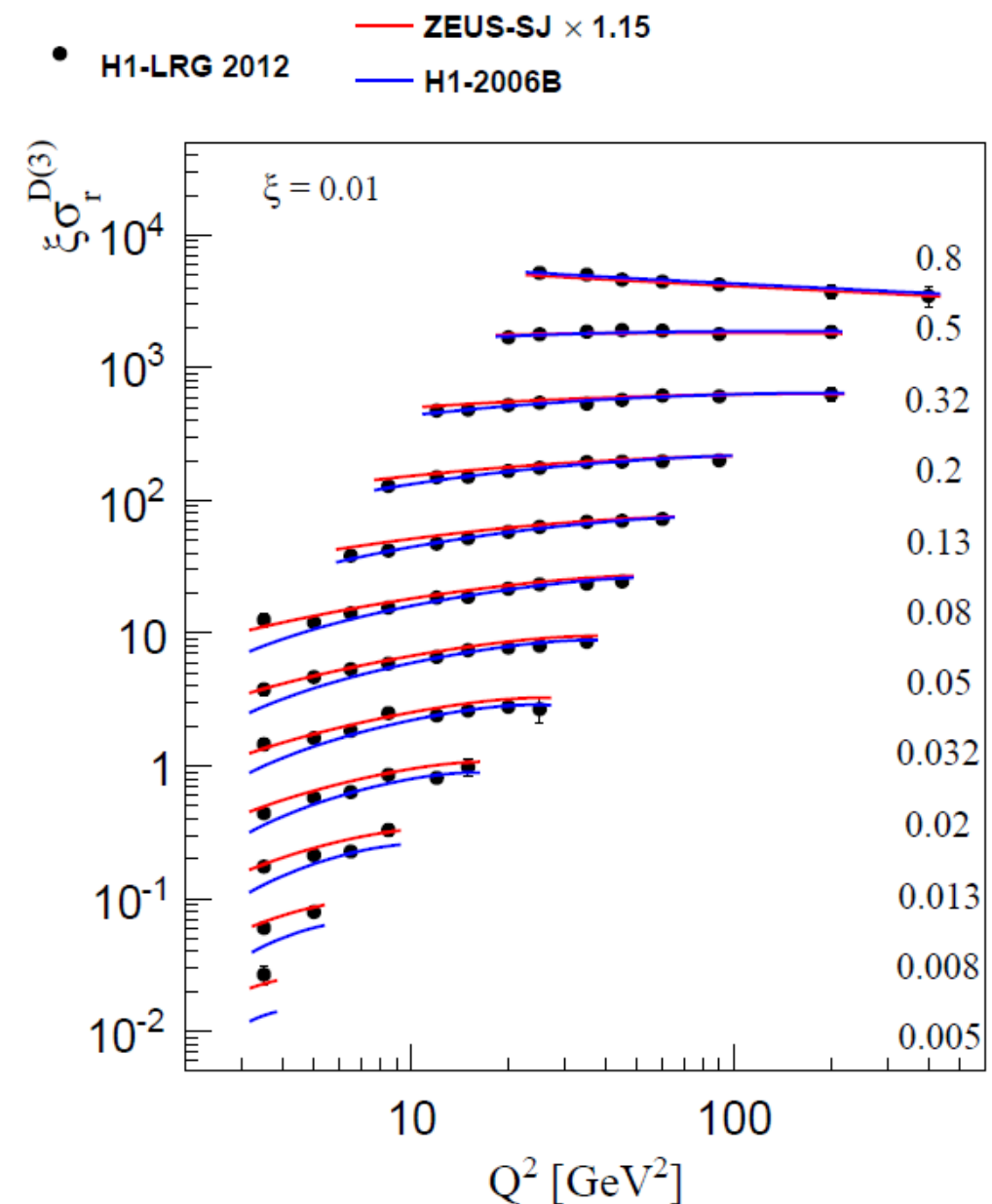
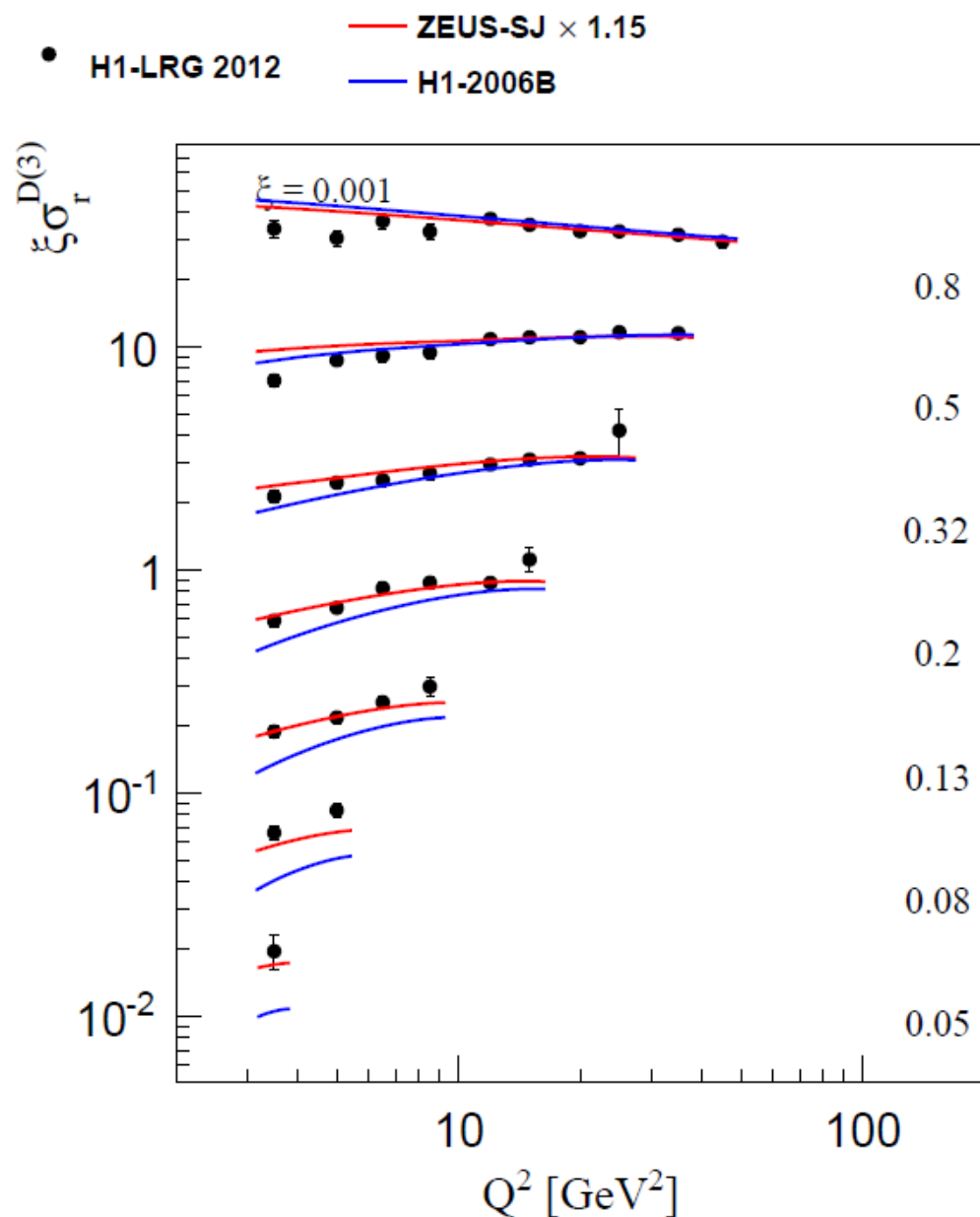
$$f_i^D(x, Q^2, x_{IP}, t) = f_{IP/p}(x_{IP}, t) f_i(\beta, Q^2) + n_{IR} f_{IR/p}(x_{IP}, t) f_i^{IR}(\beta, Q^2)$$



# Diffractive fits

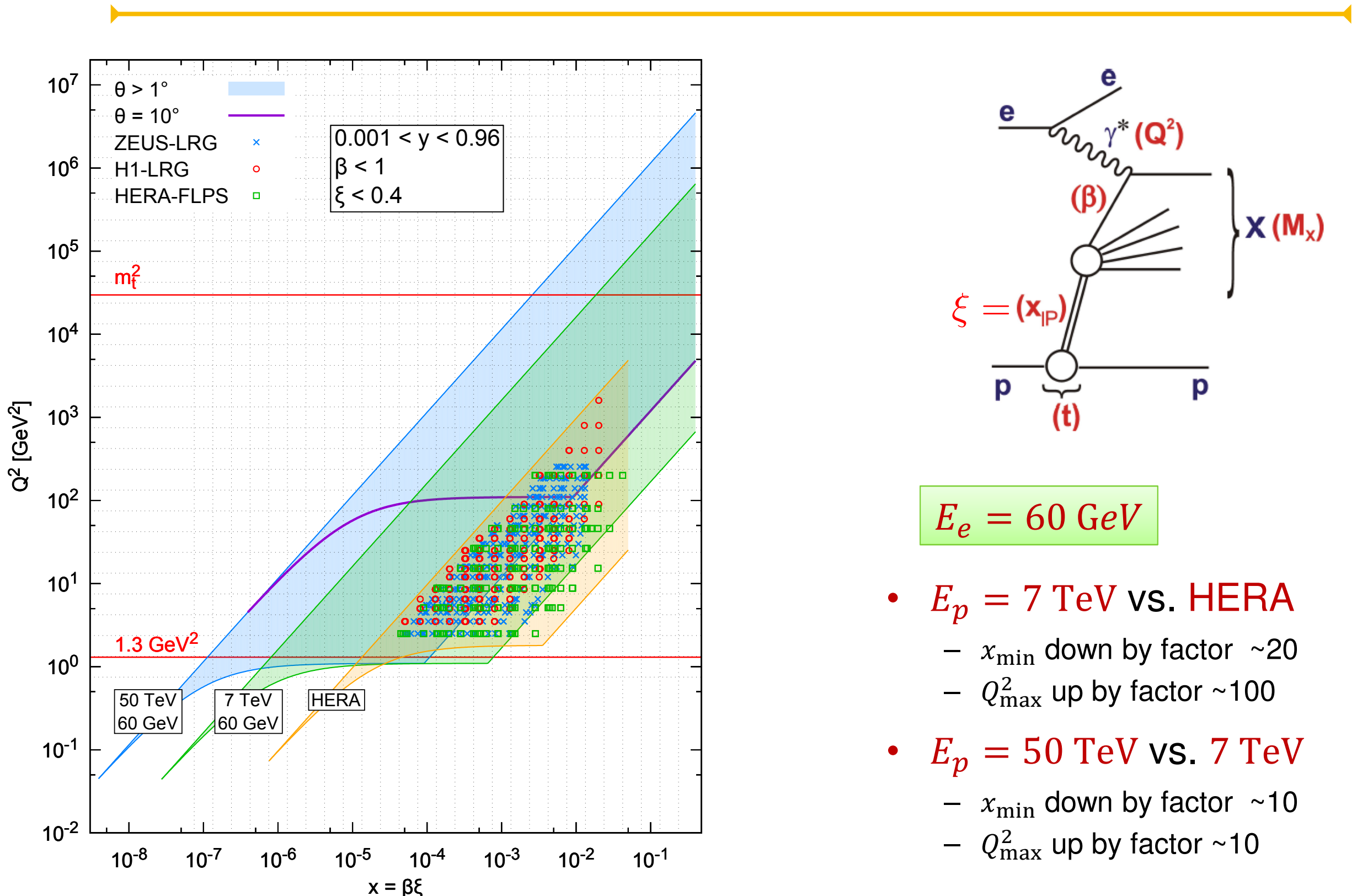
$$\xi = x_{IP}$$

Example of the DGLAP fit to the diffractive data



Comparison of H1-2006B and ZEUS-SJ fits to the H1-LRG 2012 data  
ZEUS-SJ fit seems to better describe the data in the low  $\beta$  region

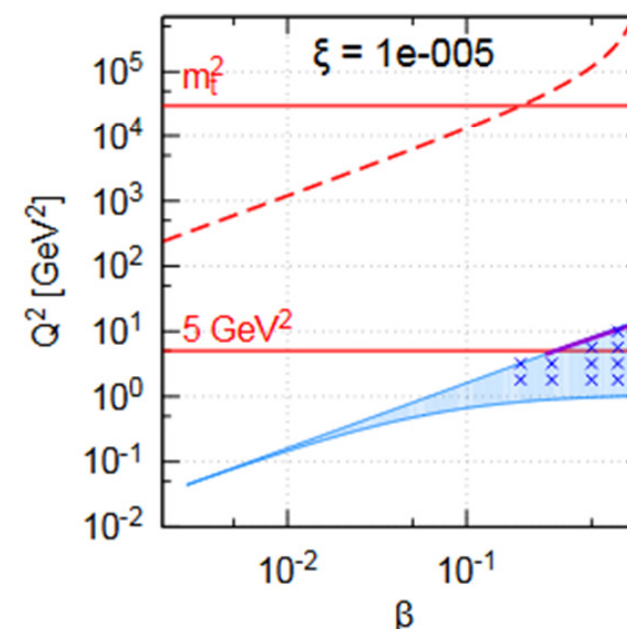
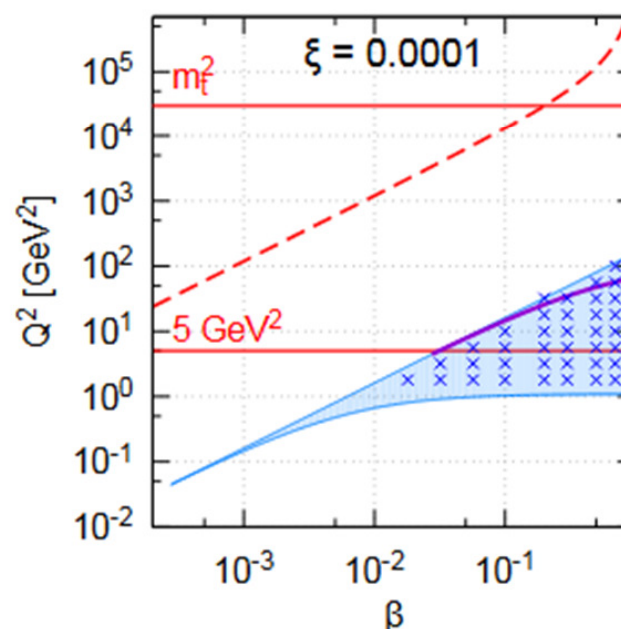
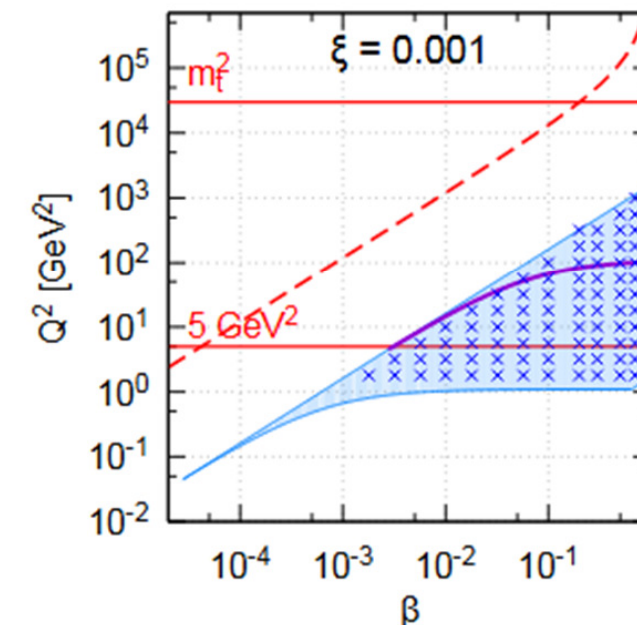
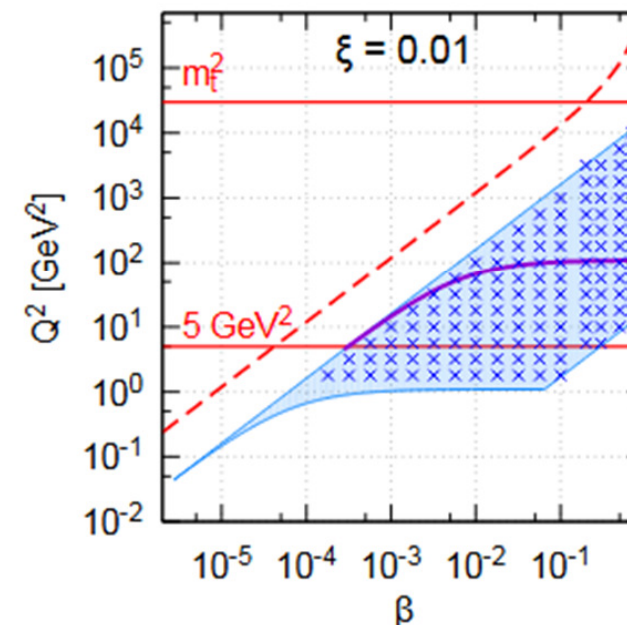
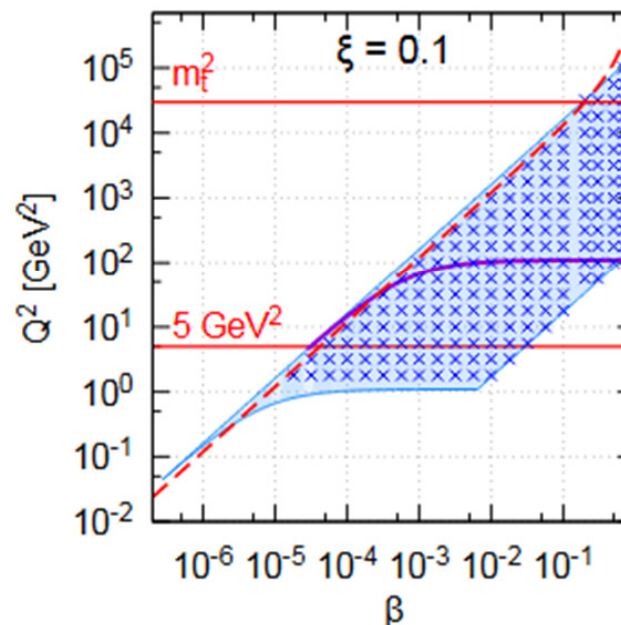
# Phase space: HERA to LHeC to FCC-eh



# LHeC phase space: $(\beta, Q^2)$ fixed $\xi$

$E_p = 7 \text{ TeV}, E_e = 60 \text{ GeV}, y_{\min} = 0.001, y_{\max} = 0.96$

$\theta > 1^\circ$   $\theta = 10^\circ$  bins  $M_X = 2 m_t$



## # bins for $\xi < 0.15$

- no top
  - 1589 for  $Q^2 > 1.3 \text{ GeV}^2$
  - 1229 for  $Q^2 > 5 \text{ GeV}^2$
- with top quark
  - 17 bins more

# FCC-eh phase space: $(\beta, Q^2)$ fixed $\xi$

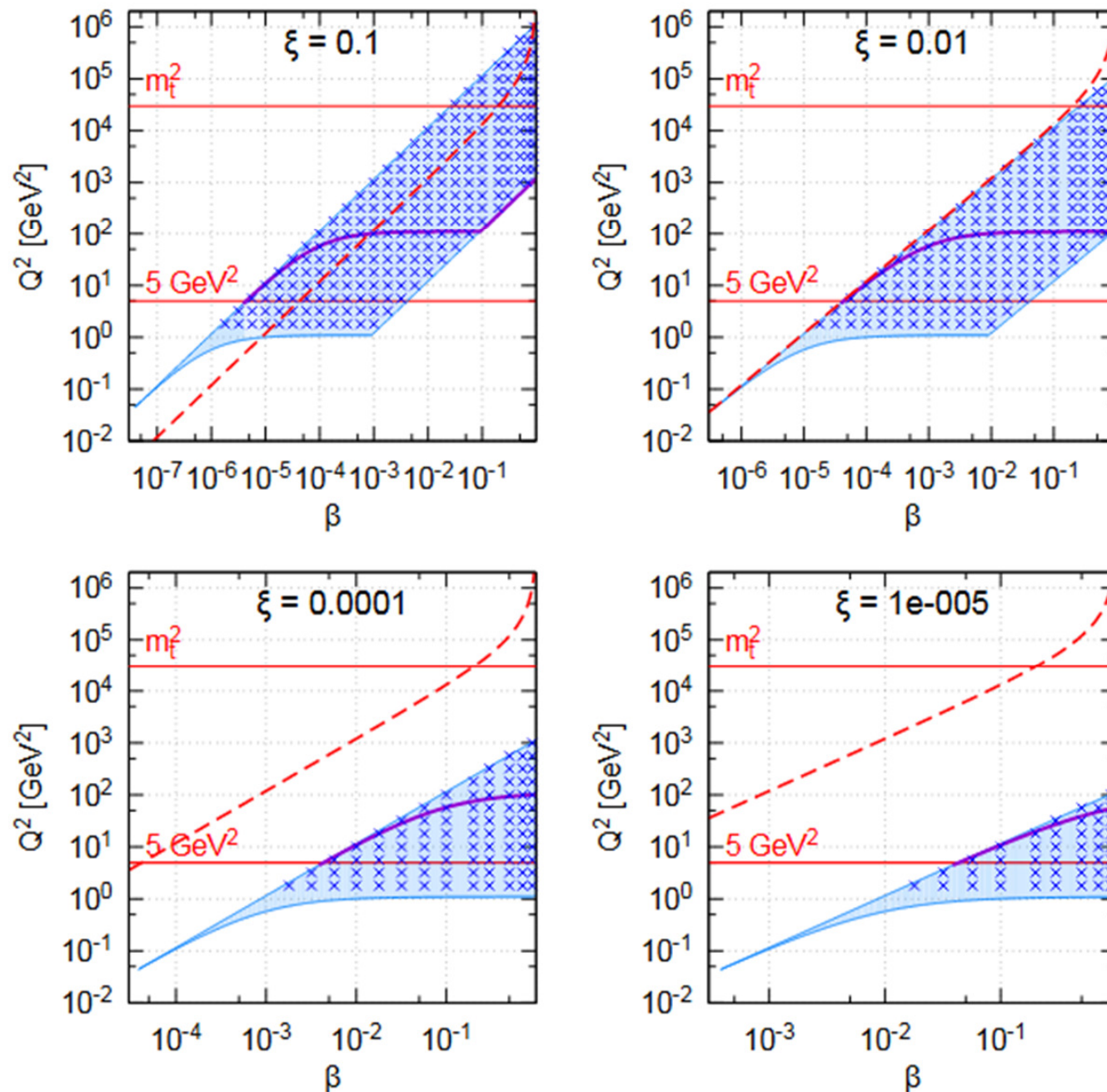
$E_p = 50 \text{ TeV}$ ,  $E_e = 60 \text{ GeV}$ ,  $y_{\min} = 0.001$ ,  $y_{\max} = 0.96$

$\theta > 1^\circ$

$\theta = 10^\circ$

bins

$M_X = 2 m_t$



## # bins for $\xi < 0.15$

- no top
  - 2171 for  $Q^2 > 1.3 \text{ GeV}^2$
  - 1735 for  $Q^2 > 5 \text{ GeV}^2$
- with top quark
  - 275 (255) bins more

# Data simulations

---

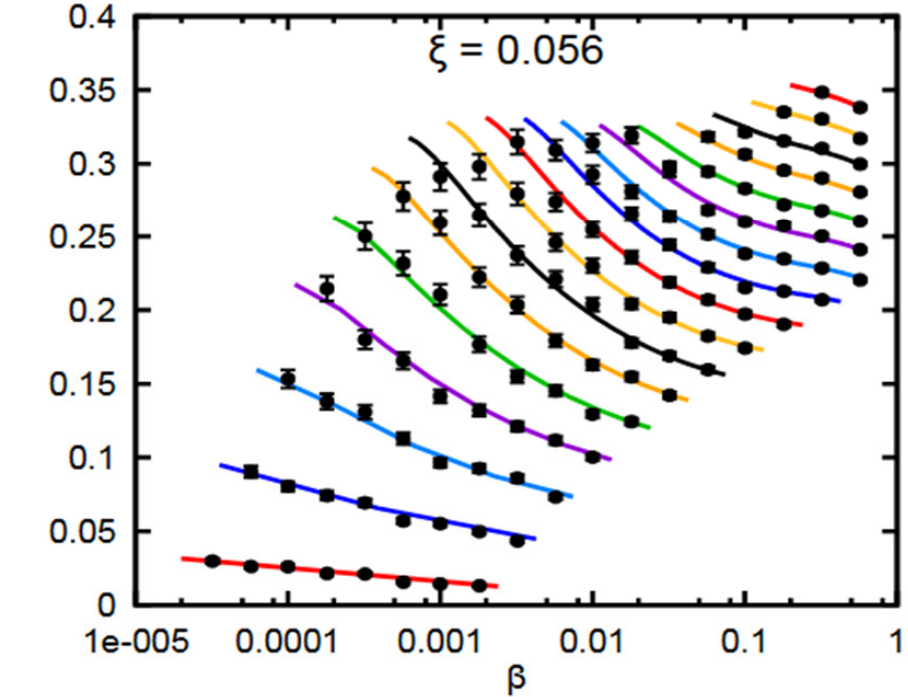
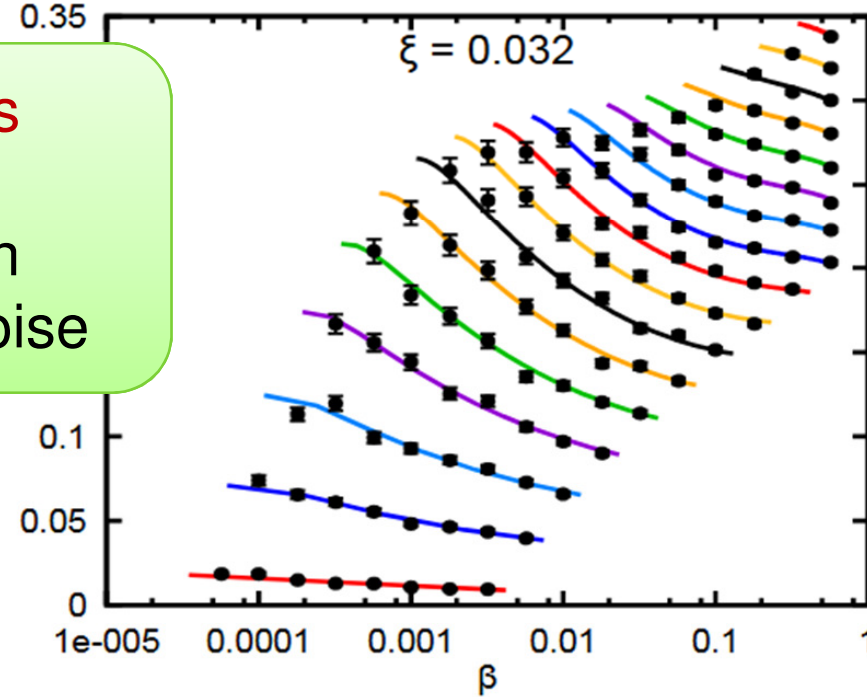
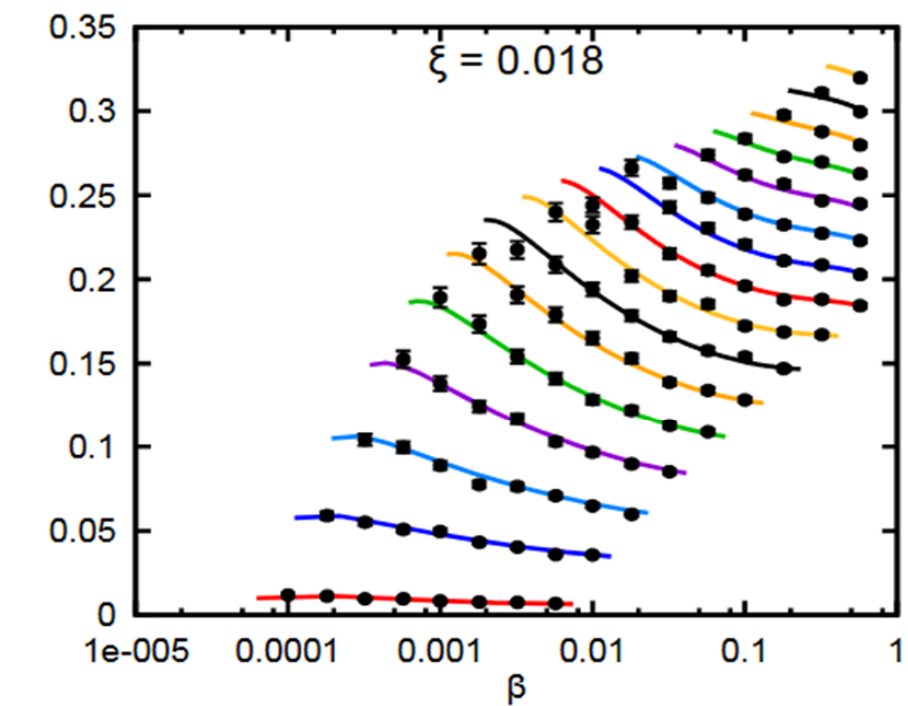
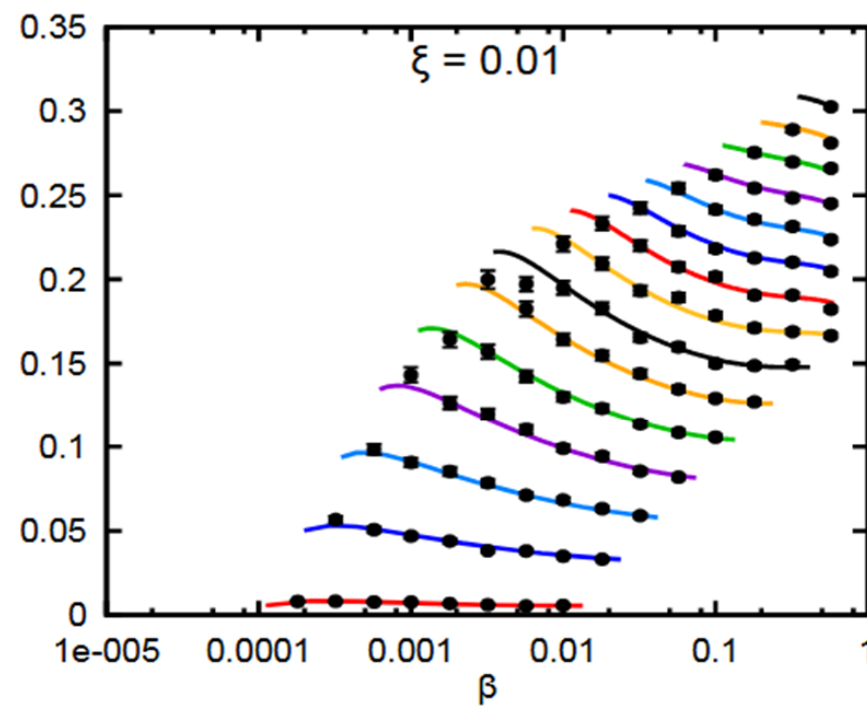
- Simulations based on extrapolation from ZEUS-SJ DPDFs
- VFNS scheme but no top at HERA so top contribution neglected in the simulation
- Errors simulated with 5% Gaussian noise
- Reggeon contribution is included but hard to constrain at HERA, could lead to large uncertainty in the extrapolation at  $\xi > 0.01$
- Binning to assume negligible statistical errors

# Example of data: large $\xi$ , LHeC

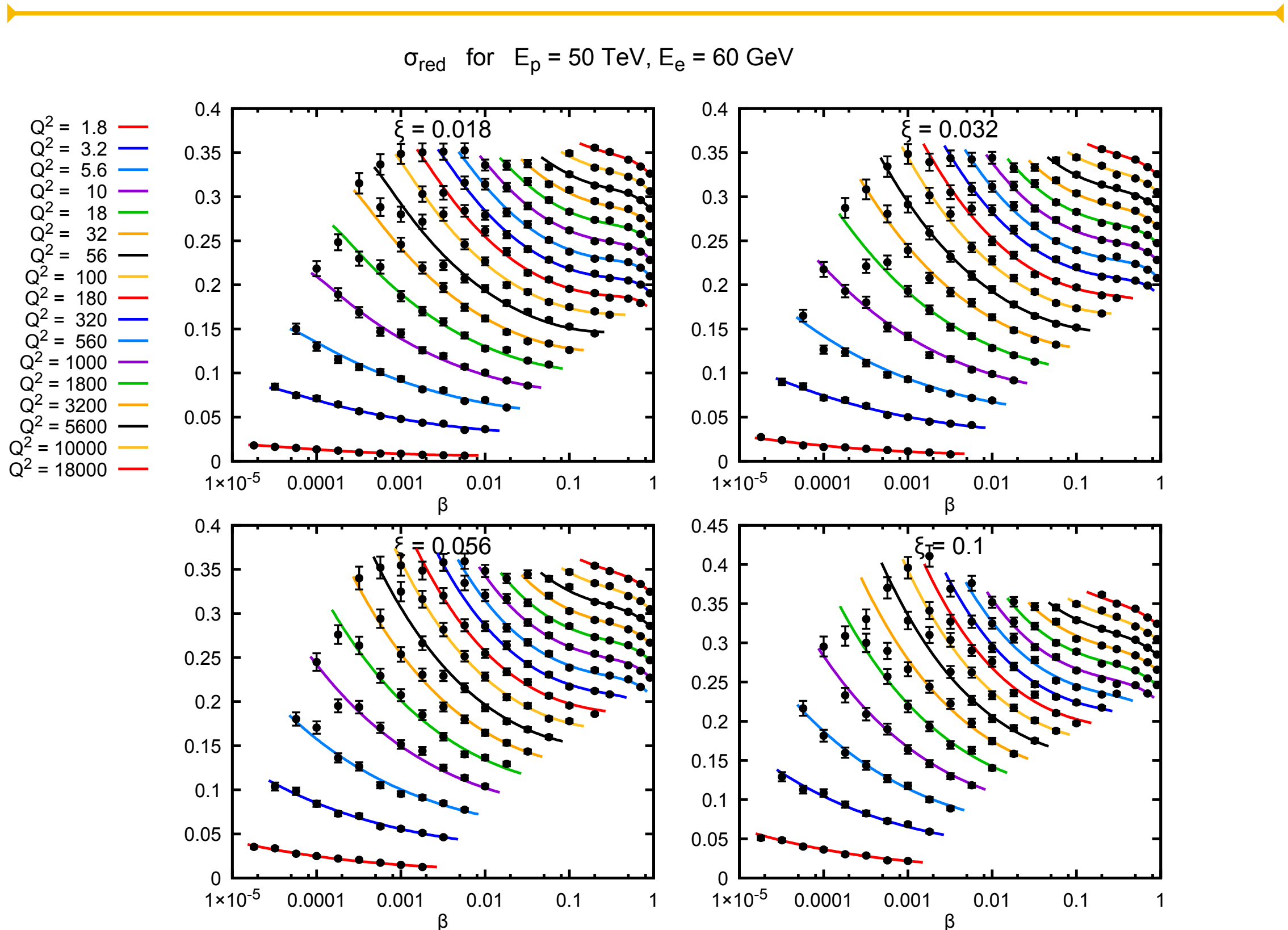
$\sigma_{\text{red}}$  for  $E_p = 7 \text{ TeV}$ ,  $E_e = 60 \text{ GeV}$

$Q^2 = 1.8$  — red  
 $Q^2 = 3.2$  — blue  
 $Q^2 = 5.6$  — blue  
 $Q^2 = 10$  — purple  
 $Q^2 = 18$  — green  
 $Q^2 = 32$  — orange  
 $Q^2 = 56$  — black  
 $Q^2 = 100$  — yellow  
 $Q^2 = 180$  — red  
 $Q^2 = 320$  — blue  
 $Q^2 = 560$  — blue  
 $Q^2 = 1000$  — purple  
 $Q^2 = 1800$  — green  
 $Q^2 = 3200$  — orange  
 $Q^2 = 5600$  — black  
 $Q^2 = 10000$  — yellow  
 $Q^2 = 18000$  — red

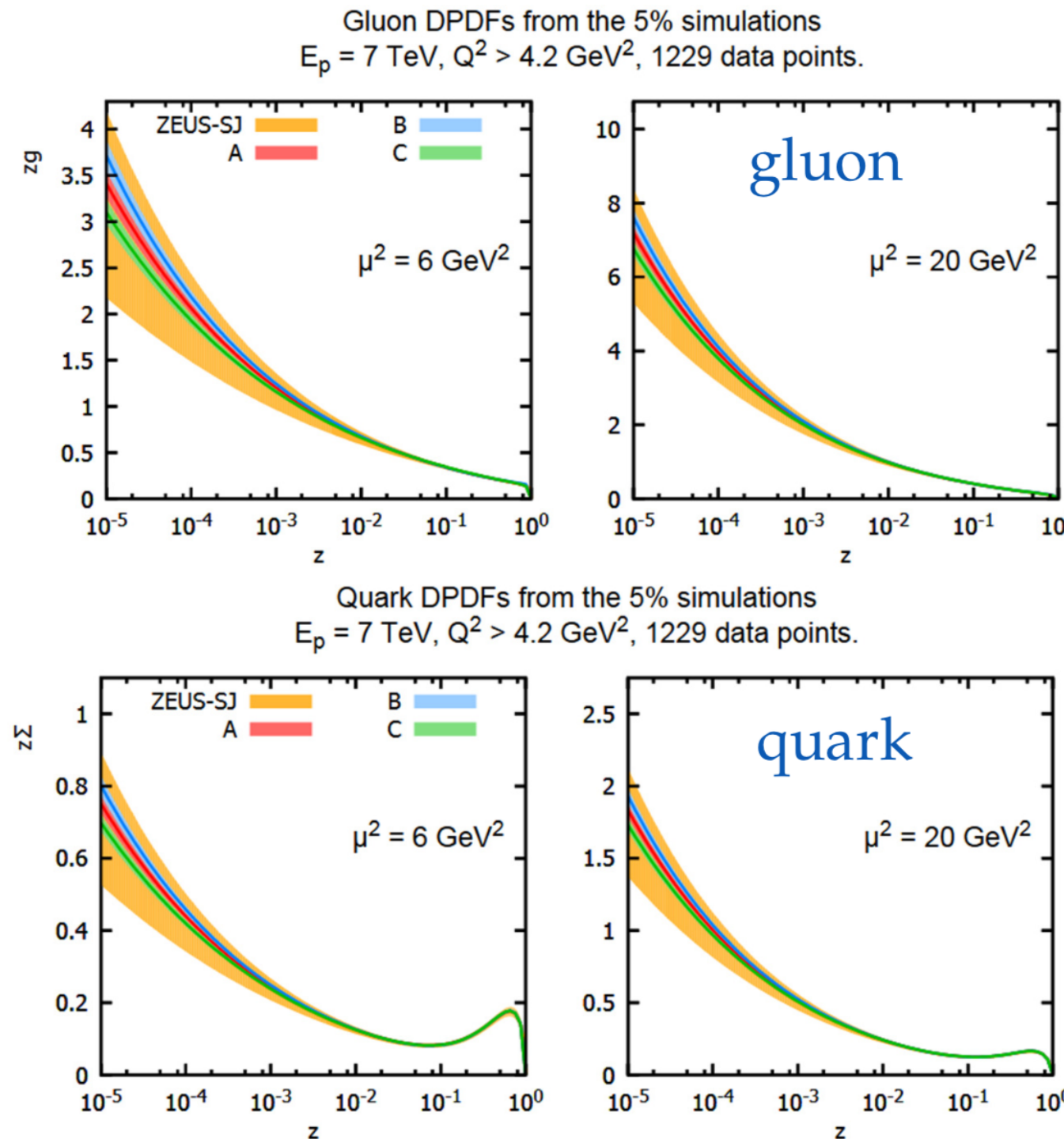
Extrapolations  
and data  
simulated with  
5% Gaussian noise



# Example of data: large $\xi$ , FCC-eh



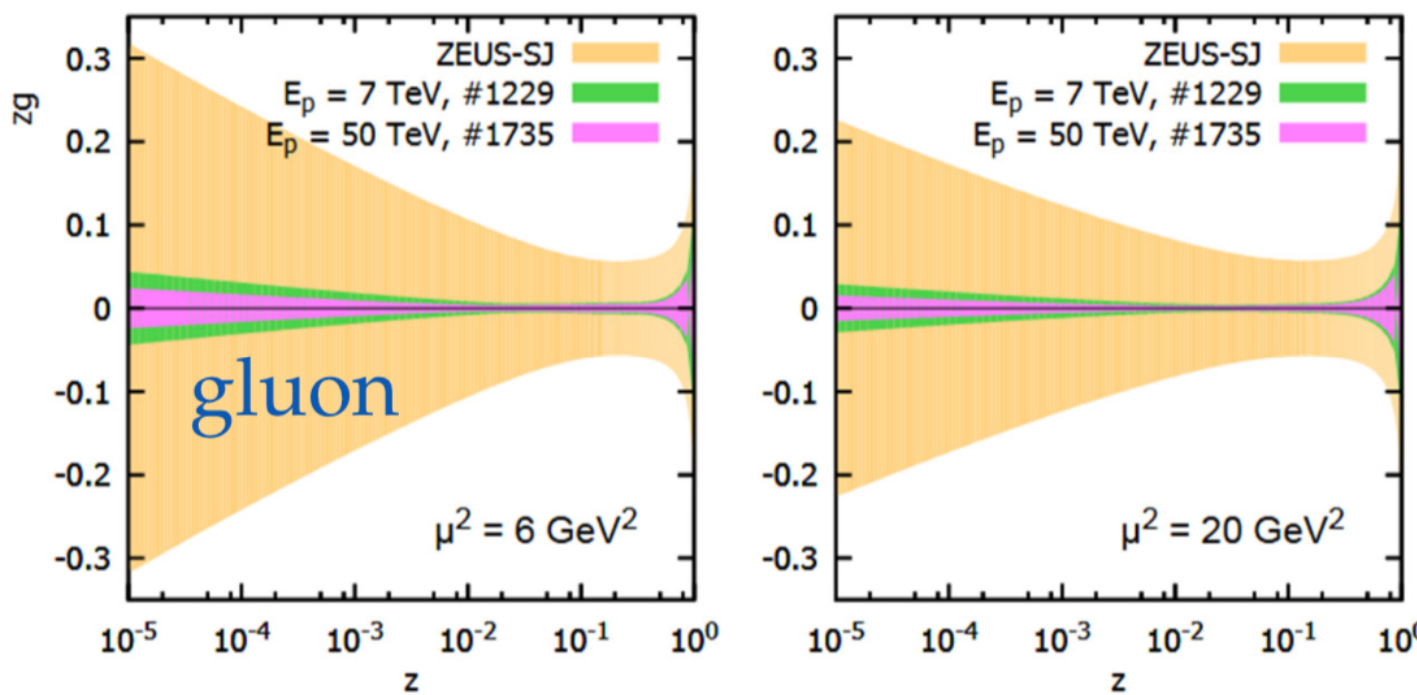
# DPDFs from simulations



$$Q_{\min}^2 \approx 5 \text{ GeV}^2$$
$$E_p = 7 \text{ TeV}$$

- Substantially improved accuracy wrt. HERA
- Statistical spread  $\sim 2 \times$  error-band
- Statistical spreads well below error-bands for  $Q_{\min}^2 \approx 1.3 \text{ GeV}^2$

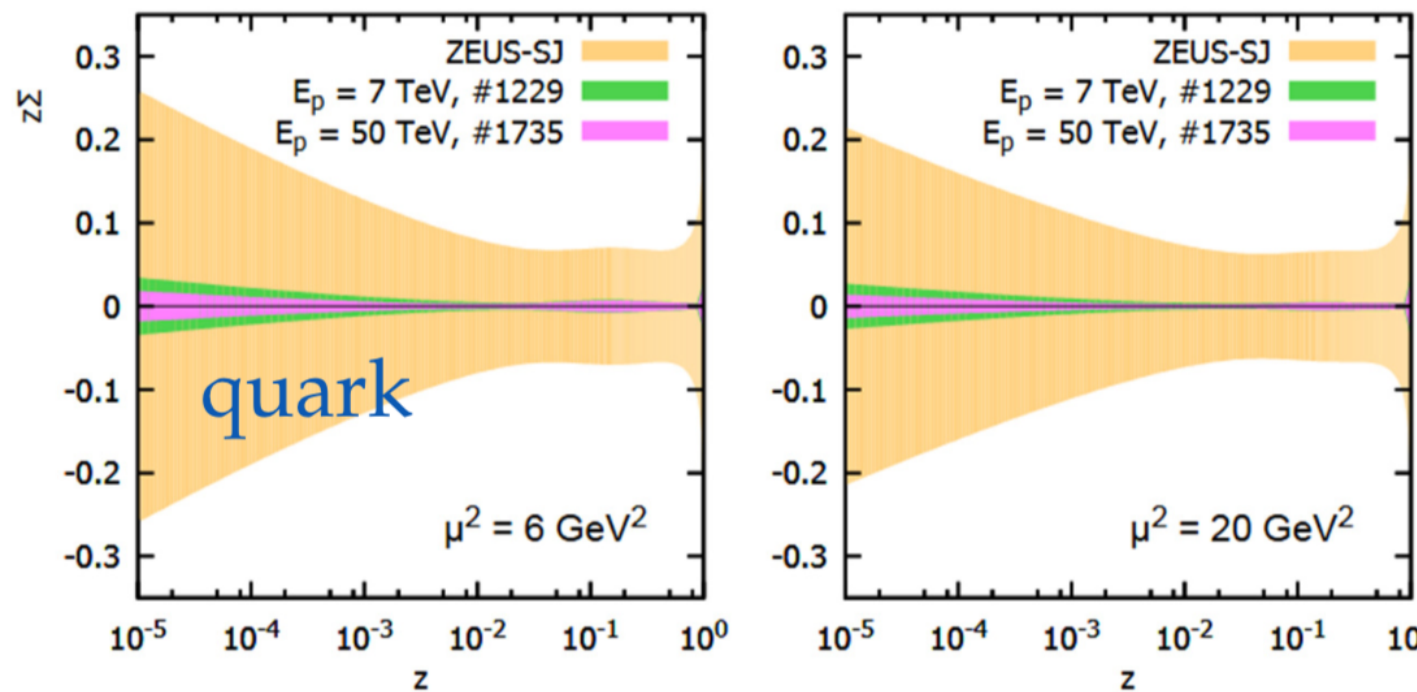
# DPDFs error bands



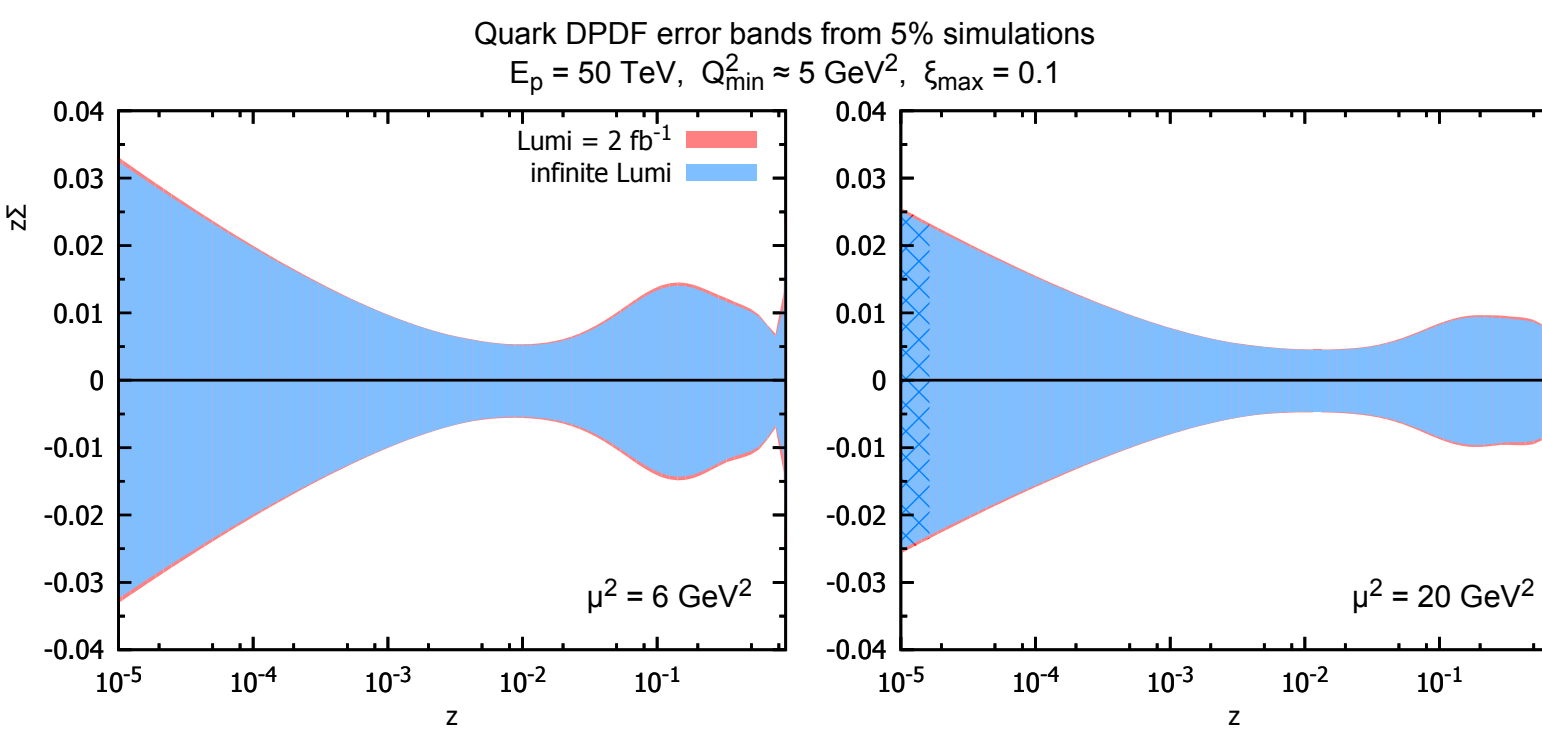
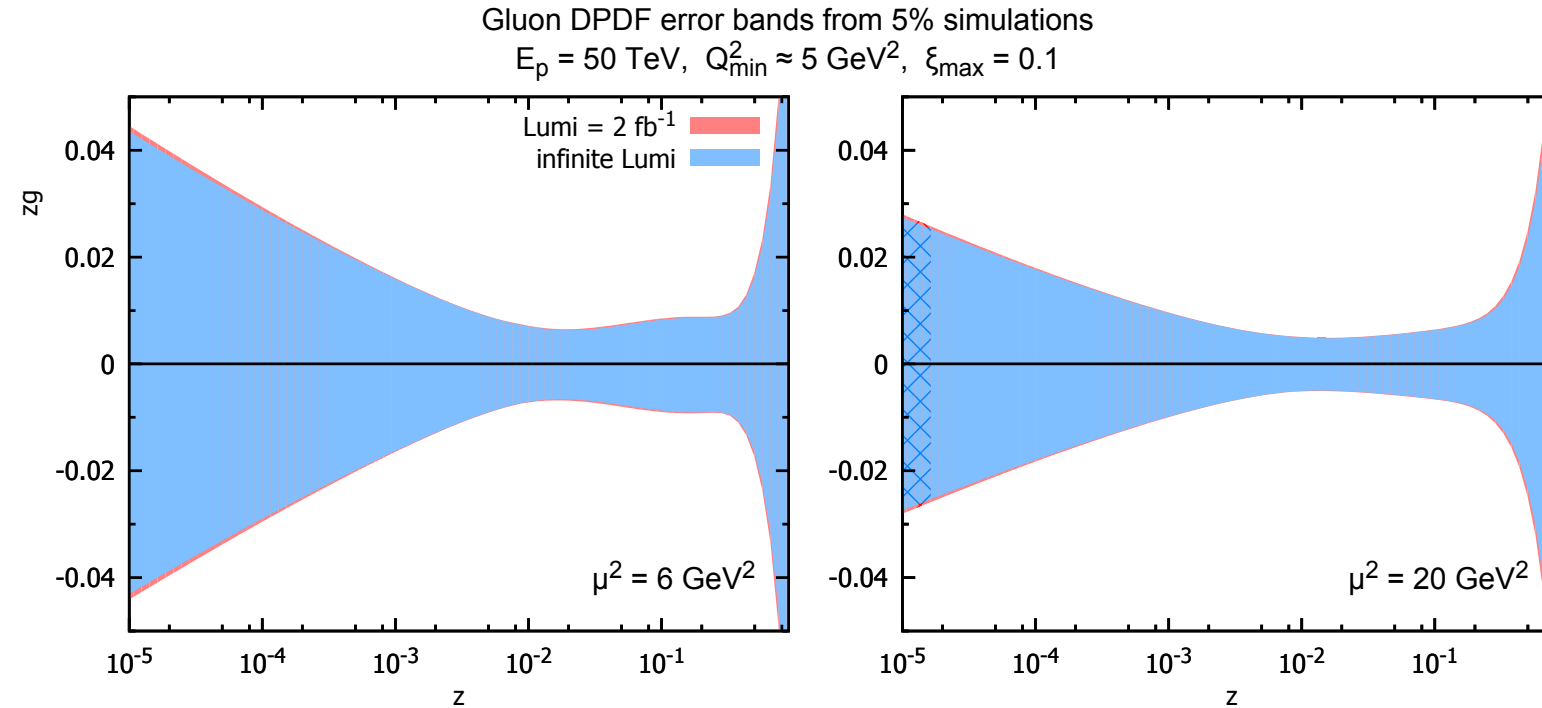
$$Q_{\min}^2 \approx 5 \text{ GeV}^2$$

Accuracy increased by

- ✓ factor  $\sim 10$  for LHeC
- ✓ factor  $\sim 20$  for FCC-he



# Luminosity study

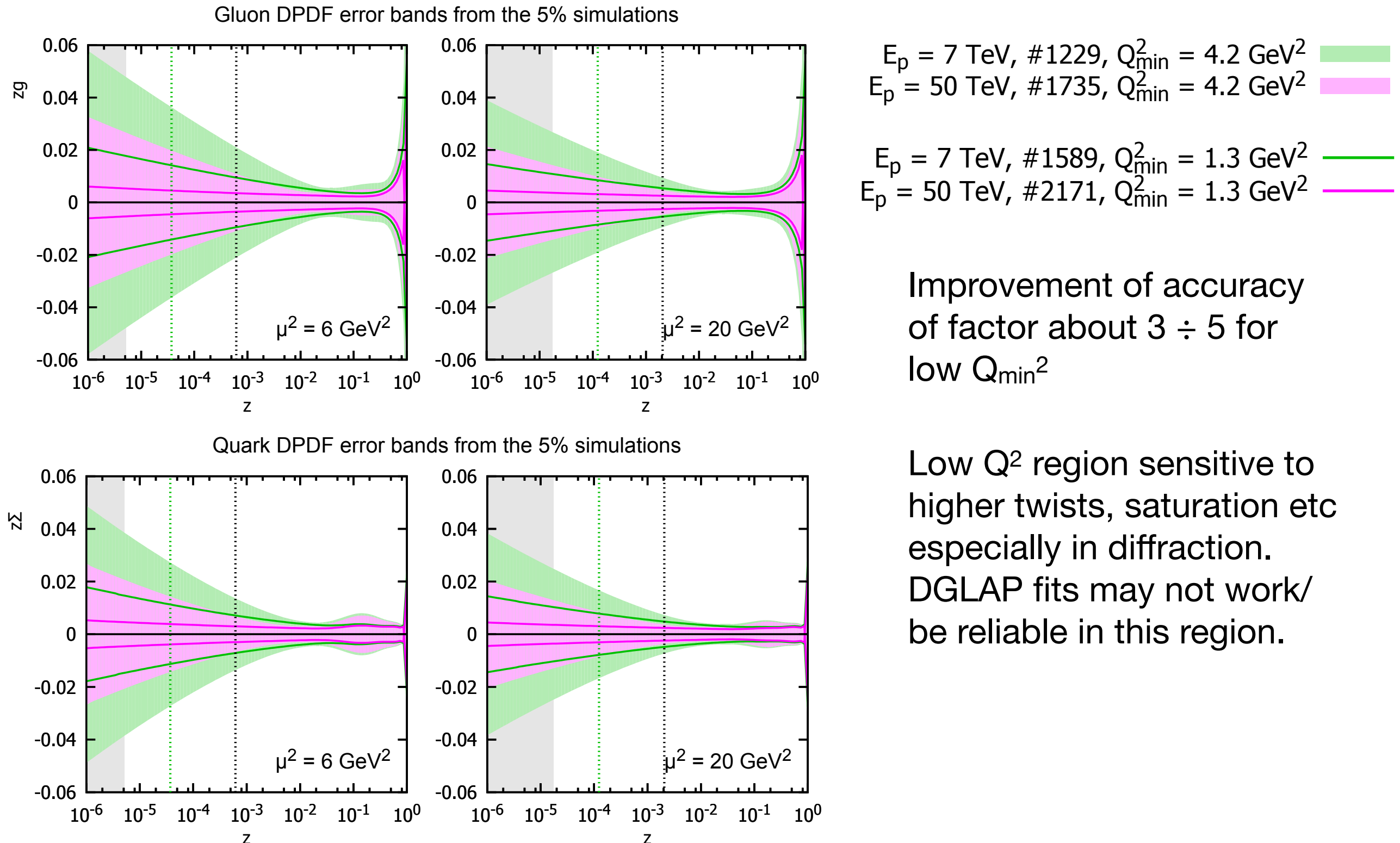


$$E_e = 60 \text{ GeV}$$
$$E_p = 50 \text{ TeV}$$
$$Q^2_{\min} \simeq 5 \text{ GeV}^2$$

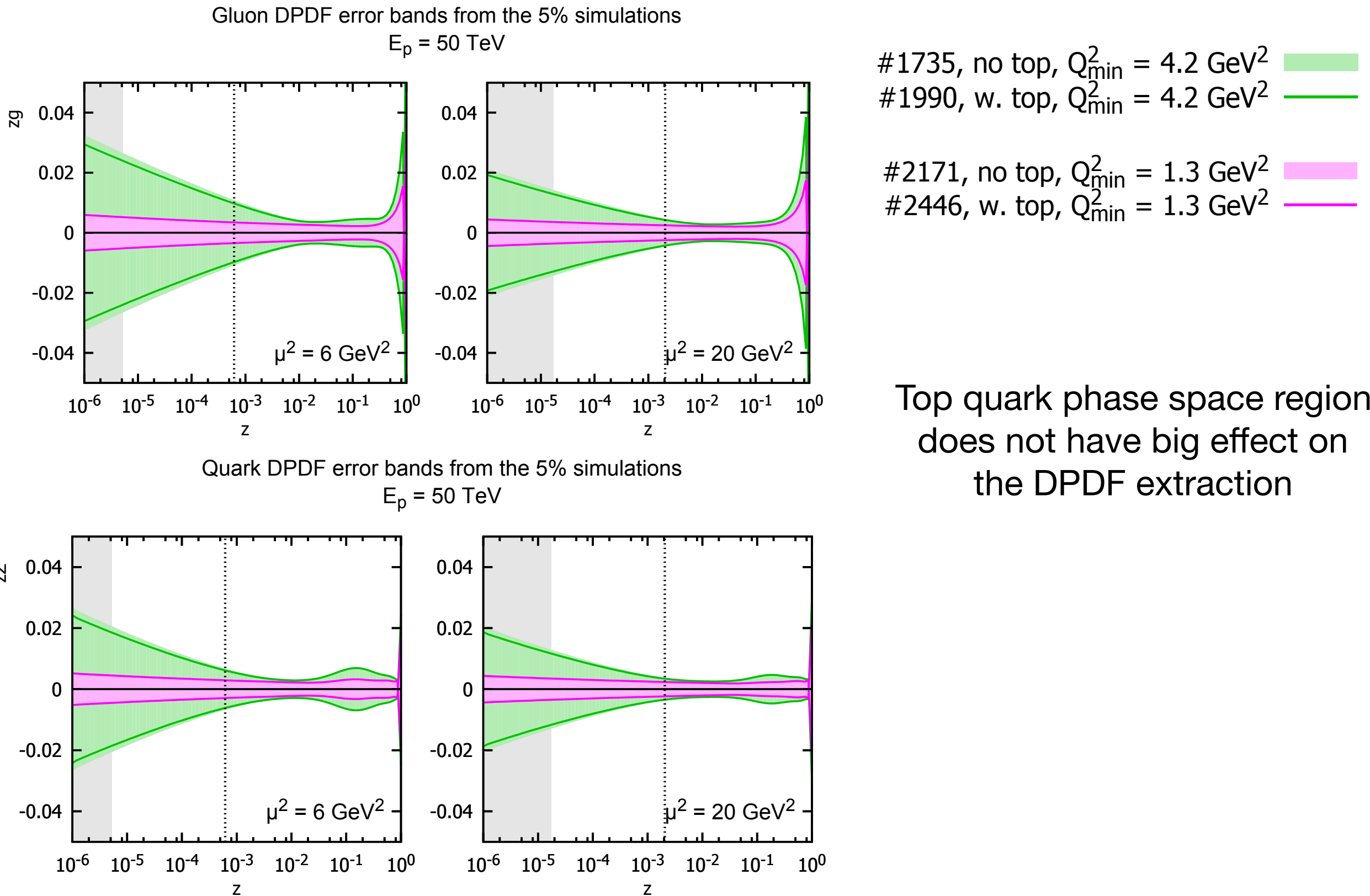
Comparison of ‘infinite’  
Lumi simulation and  
Lumi= $2 \text{ fb}^{-1}$

For this measurement there  
is negligible difference

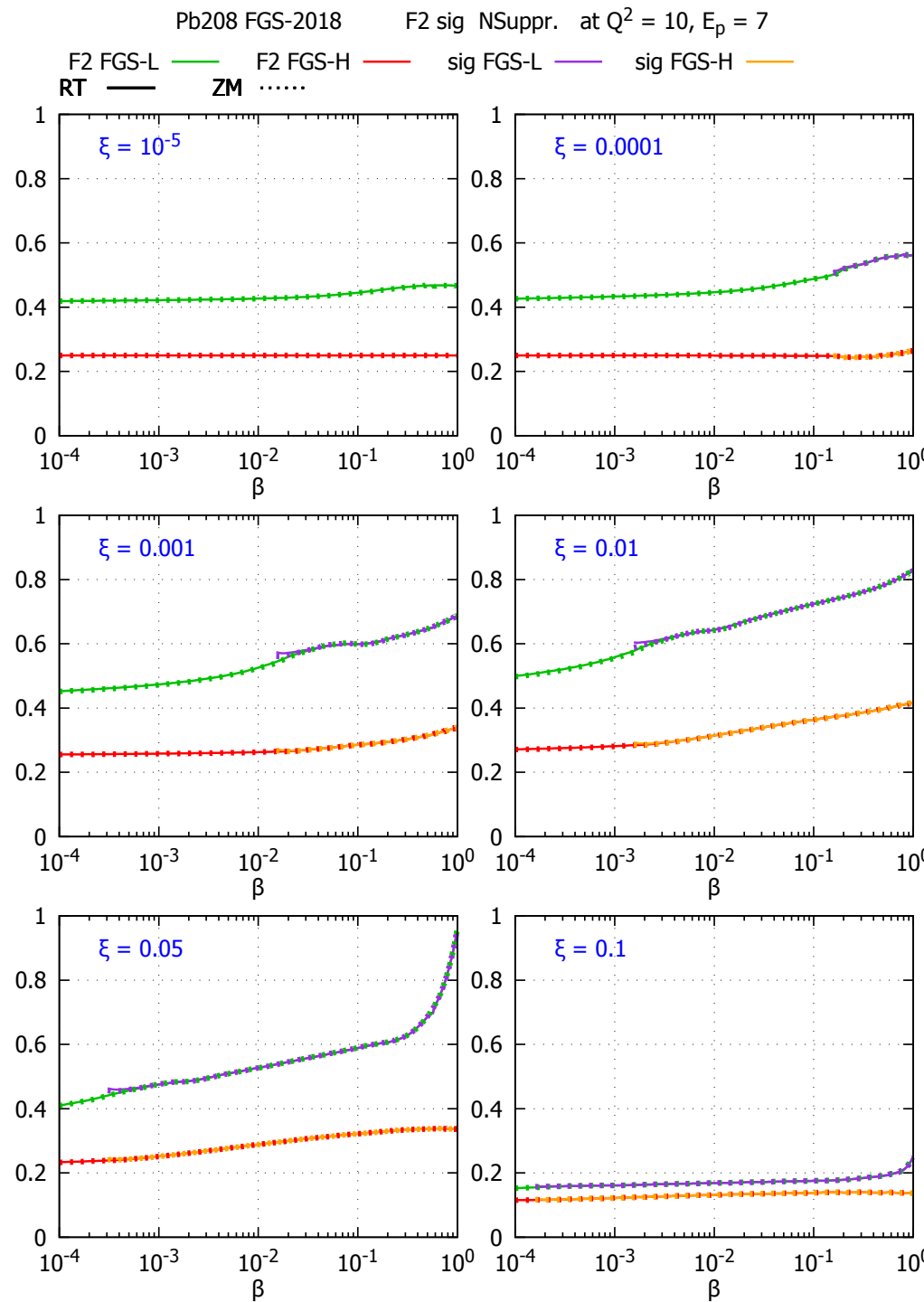
# Dependence on $Q_{\min}^2$ and $E_p$



# DPDF accuracy: top contribution



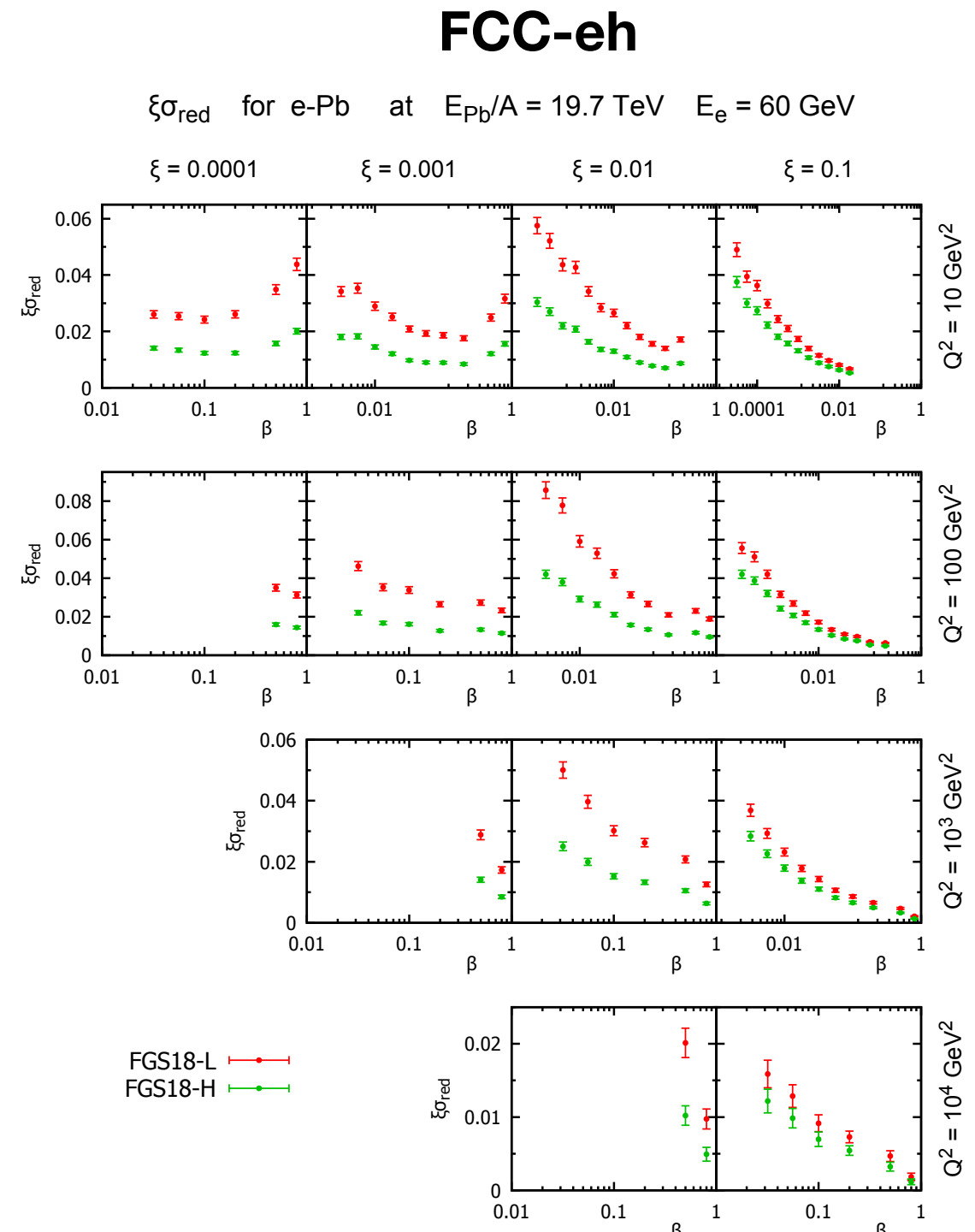
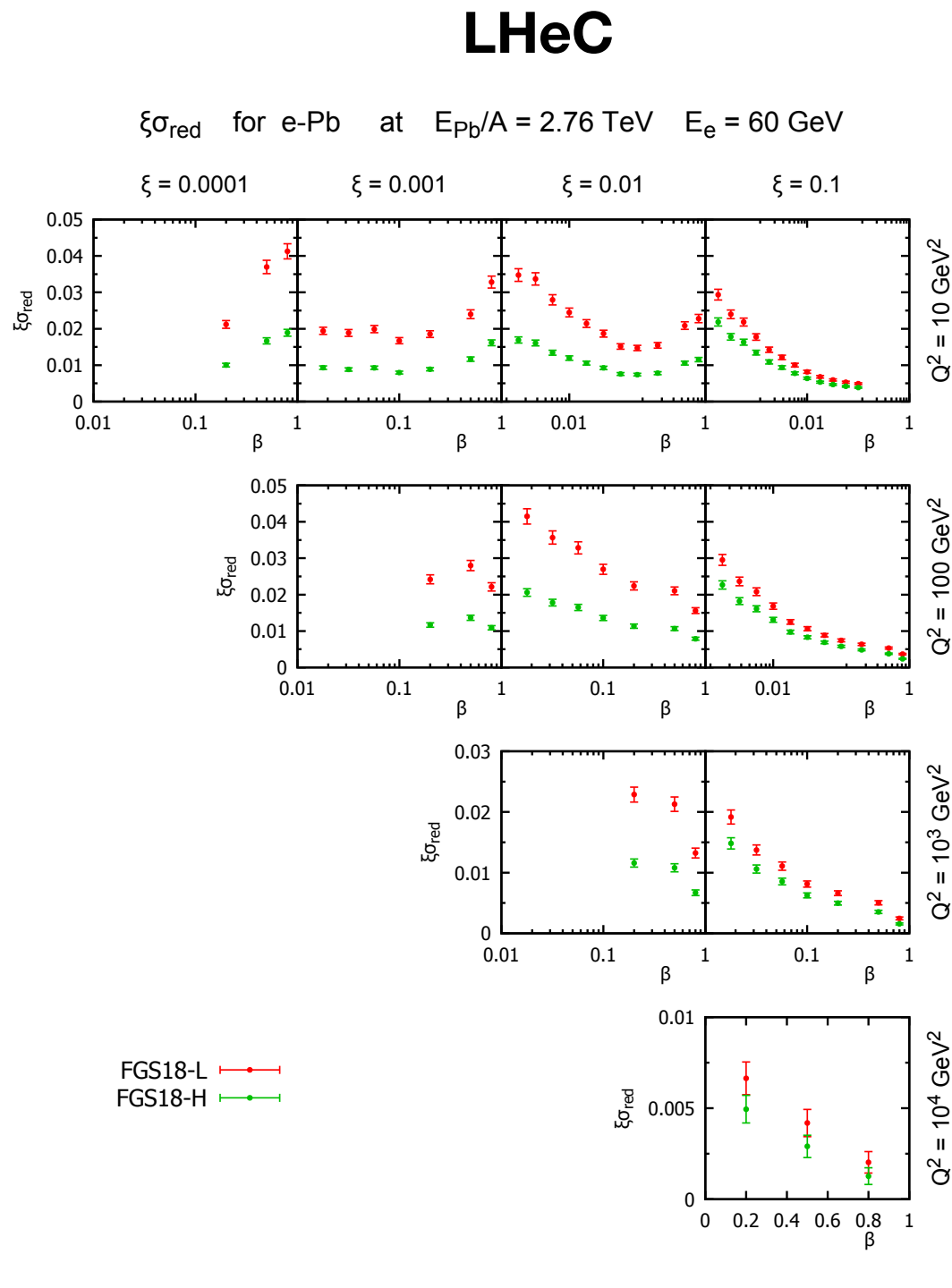
# Nuclear diffractive structure functions



- Model for nuclear shadowing: Frankfurt,Guzey,Strikman
- Two models: high and low shadowing
- Results for nuclear ratio:

$$R_k(\beta, \xi, Q^2) = \frac{f_{k/A}^{D(3)}(\beta, \xi, Q^2)}{A f_{k/p}^{D(3)}(\beta, \xi, Q^2)}$$

# Nuclear diffractive cross sections



# Summary and Outlook

---

- New possibilities for studies of diffraction at LHeC and FCC-eh.
- DPDF accuracy increased by about factor 10 at LHeC and 20 at FCC-eh.
- It is possible to constrain gluon by inclusive data alone. Diffractive dijet production was necessary at HERA to constrain the gluon, such constraints could also be included at LHeC/FCC-eh further reducing accuracy.
- Possibility of producing diffractive top. DPDF determination does not seem to be affected much by the top though.
- Lowering initial  $Q^2$  increases the accuracy. This is the region that is expected to be very sensitive to higher twists in diffraction. Further analysis with better modeling of this region is necessary to estimate the impact of such correction.
- First analysis for diffraction in e-Pb at LHeC/FCC-eh.